An Approximate Effective Index Model for Efficient Analysis and Control of Beam Propagation Effects in Photonic Crystals

Babak Momeni, *Student Member, IEEE, Member, OSA,* and Ali Adibi, *Senior Member, IEEE, Member, OSA*

***Abstract*—Propagation of optical beams through a photonic crystal (PC) is analyzed and modeled. It is shown that the propagation effects for beams with slow spatial variations can be effectively modeled by diffraction behavior obtained directly from band structure. In particular, we present here an approximate model based on defining an effective index for the PC that can be used to analyze the propagation of optical beams inside the PC using the well-known analytic formulas for wave propagation in bulk media. The model presented here allows for considerable reduction in computation time and complexity. It also allows us to obtain more intuitive and design-oriented information about beam propagation effects inside PCs. We apply this model to several practical cases and show that its results agree very well with direct (time-consuming) numerical simulations.**

***Index Terms*—Diffraction, effective index, periodic structures, photonic crystals (PCs), propagation.**

I. Introduction

PHOTONIC crystals [1], [2] have inspired a lot of research recently due to their ability to control the propagation of electromagnetic waves. The majority of investigations on photonic crystals (PCs) have been devoted to their photonic bandgap (PBG) and possible applications arising from that, such as suppressing spontaneous emission [1], realizing waveguides and bends [3]–[5], and microscale cavities [6]. Propagation of waves in a one-dimensional (multilayer) photonic crystal has been investigated in applications like pulse compression [7], [8] and spatial beam shaping [9]. Only recently, the propagation of electromagnetic waves with frequencies outside the PBG in two-dimensional photonic crystals has been proposed for exploiting other capabilities of photonic crystals for new applications [10]–[12]. An example is the superprism effect that has been proposed [13] based on the anomalous dispersion of photonic crystals and implemented in planar structures [14], [15]. Some issues about efficiency of wavelength demultiplexers based on the superprism effect have been discussed in [16]–[18]. Another possible application of the dispersion properties of PCs out of the PBG is beam coupling to planar structures [19] in which a photonic crystal structure is used to make the coupling of an optical beam to a planar structure possible. Furthermore, beam-collimation for guiding [20]–[24] and for controlling the behavior of beams generated by sources inside the photonic crystal has been proposed. Another application is based on heterostructure photonic crystals [25] in which PCs are considered as media with partially controllable properties and waveguiding is made possible by combining appropriate regions of different photonic crystals.

In applications involving propagation of light beams through PCs, the actual beam shapes and the corresponding propagation effects in large PC structures should be considered. To analyze the propagation effects, we need to monitor the propagation over a large area of the structure, which needs a huge amount of computation using conventional direct electromagnetic wave simulators like finite-difference time domain (FDTD) [26], time-domain beam propagation method (TD-BPM) [27], and multiple scattering technique [28]. Spectral methods based on modal expansion of the field are advantageous for the analysis of these structures [29], but an approximate method which gives insight into the beam propagation process will be helpful to avoid a mass of computations for each particular case. To the best of our knowledge, there has been no report on such an approximate technique. In this paper, we investigate these propagation effects inside PCs using modal expansion and derive a simple (approximate) effective index model for the range of beams which are mainly used in the applications mentioned above. We show that an effective index model only requires numerical simulation for the calculation of band structure, which is typically performed by analyzing only a unit cell of the PC. After finding the effective index, the propagation of electromagnetic waves inside the PC can be analyzed using the well-known analytic formulas for bulk media. Thus, the effective index model proposed here reduces the computation time for the analysis of electromagnetic wave propagation inside PCs by several orders of magnitude. Using this model, we also explain how diffraction control devices can be implemented by designing proper PC structures.

In Section II, we briefly review the anomalous dispersion properties of PCs outside the PBG. The proposed approach for the approximate analysis of beam propagation inside PCs is explained in Section III, and the effective index model is derived in Section IV. The applications of the effective index model to several practical applications of the PCs are discussed in Section V. The validity of the model and its possible extensions are discussed in Section VI. Final conclusions are made in Section VII.

Manuscript received April 5, 2004; revised November 4, 2004. This work was supported by the Office of Naval Research and by the Air Force Office of Scientific Research.

The authors are with the School of Electrical and Computer Engineering, Georgia Institute of Technology, Atlanta, GA 30332 USA.

Digital Object Identifier 10.1109/JLT.2004.841444

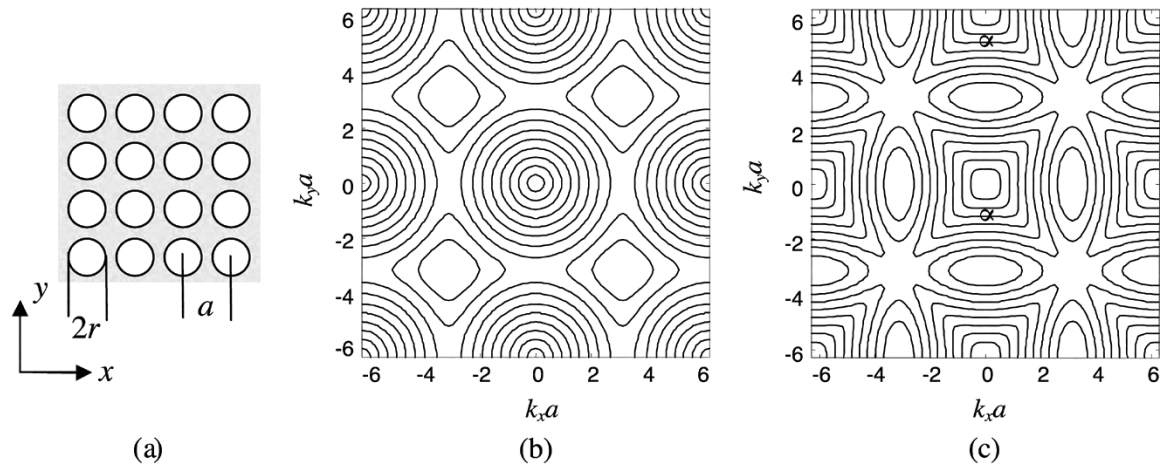

Fig. 1. (a) Square lattice PC of air-holes in Si. Constant frequency contours with TE polarization are shown in the (b) first band and (c) second band for $r/a = 0.40$.

II. Anomalous Dispersion in Photonic Crystals

Unlike the dispersion in nondispersive bulk materials, the wavenumber-frequency relation in photonic crystals is not linear even when the PC is made of linear nondispersive dielectrics. The reason is obvious because the frequency (or ω) of each PC mode has to be periodic in wavevector (or k) domain [30]. Moreover, unlike material dispersion, which typically introduces small perturbation to linear dispersion (i.e., $\omega = ck$, with c being the speed of light in the material), the modal dispersion caused by nonhomogeneity of the PC structure usually results in much stronger nonlinearity in the dispersion behavior. Due to their large permittivity contrast, the PCs are highly dispersive with the effect being stronger at higher frequencies.

Fig. 1(a) shows a typical two-dimensional (2-D) PC of air cylinders with radius r and period a in Si ($\varepsilon_r = 11.4$). The first two bands of the band structure of the PC in Fig. 1(a) for $r = 0.4a$ are shown in Fig. 1(b) and (c), respectively, in the form of constant frequency contours in the 2-D k-space. As can be seen in Fig. 1(b) and (c), the periodicity of the band structure imposes some deviations from normal bulk band structure (i.e., circular constant frequency contours in the form of $\omega = c|\bar{k}| = c\sqrt{k_x^2 + k_y^2}$) especially at the edges of the Brillouin zone. If we concentrate on the second band [Fig. 1(c)], it is seen that at relatively small values of k_x and k_y (for example, $k_x a, k_y a < \pi$), the constant frequency contours are considerably different from the bulk (circular) dispersion behavior. These regions are the regions with large anomalous dispersion properties in the photonic crystals. Of these properties, for example, we can consider the flat (horizontal) regions of the band structure, specified by α in Fig. 1(c). As shown before, such points in the band structure correspond to photonic crystal modes propagating in y-direction with very small diffraction inside the structure [22], [23].

III. Approximate Analysis of Beam Propagation Inside PCs

To analyze the propagation of a finite-size beam in space, the best way is to make use of its analogy with the well-developed time-domain pulse propagation [31]. The analogy relates space and spatial frequency of a finite-size beam to time and temporal frequency, respectively, of a pulse in time-domain. In this view, the variation of beam shape during propagation is mainly due to changes either in the amplitude or in the phase of the spectral content of the beam. For example, spectral phase is responsible for beam shape variations during propagation in a lossless bulk material where the spectral content amplitude of the beam is conserved.

In this paper, we investigate the effect of propagation on the spatial shape of the optical beams. Thus, spectrum throughout this paper refers to the spatial spectrum of the beam under consideration, unless otherwise stated. The relation between the spatial content (i.e., $p(x)$) and spectral content $(P(k))$ of an optical beam profile in one dimension (x) is obtained by spatial Fourier transformation

$$P(k) = \int p(x) \exp(-jkx)\, dx. \tag{1}$$

For this paper, we limit our discussion to propagation in 2-D problems, and monitor the beam profile along some lines inside the structure. Assume $P_i(k)$ is the spectral representation of a monochromatic beam at position i, where k is the spatial frequency corresponding to the spatial coordinate normal to the propagation direction in a 2-D structure. Since the propagation is a linear process, its effect on the spectrum of a beam propagating from an arbitrary plane 1 to another plane 2 can be modeled simply by a transfer function $H(k)$ as

$$P_2(k) = H(k)P_1(k). \tag{2}$$

If the excitation is relatively narrow-band around $k = k_c$ in k domain, and the propagation characteristics of the structure (i.e., the band structure in the PC case) are smooth in the excitation bandwidth, the function $H(k)$ can be approximately represented by the first three terms of its Taylor expansion

$$H(k) \cong \exp\{-j[\Phi_0 + (k - k_c)\Phi_1 + (k - k_c)^2\Phi_2]\}. \tag{3}$$

Here we assume the medium to be lossless resulting in unity amplitude for $H(k)$. The effect of each of these three terms

on the propagation of a beam can be separately studied. The zeroth-order term is simply a constant phase change in the resulting beam and can be neglected since it does not have any effect on the beam shape. The first-order spectral phase term (involving Φ_1) adds a linear phase (i.e., $(k - k_c)\Phi_1$) to the beam spectrum that results in a shift in space. This term is actually responsible for the drift of the beam from its original coordinate. The second-order spectral phase term (involving Φ_2) adds chirping to the beam spectrum, resulting in broadening of the beam in space [31]. Again it is worth noting that this term is constant for each temporal frequency in different directions in ordinary homogeneous isotropic media, and decreases as the frequency is increased. We limit our treatment of beam propagation effects to these terms and consider higher order effects as perturbations to this model.

To investigate the effects of beam propagation through PCs, two basic questions arise. First, what happens when an ordinary light beam from a homogeneous medium gets to an interface with a photonic crystal (i.e., analysis of transmission through the interface)? Second, having an initial field profile inside the photonic crystal, how does propagation through the PC affect it (i.e., analysis of beam propagation)? In the following section, we will address these questions.

IV. Effective Index Model for the Analysis of Beam Propagation in Photonic Crystals

Since we intend to develop an approximate model for beam propagation inside the PCs, we first clarify the assumptions of the model. The first assumption is that the beam has a relatively narrow spectral content in the sense that the Taylor approximation in (3) acceptably represents the behavior of the PC structure in the spectral range that the beam has appreciable content. The second assumption is that we are working in single-mode region of the PC. It means that for each plane-wave component of the incident beam at the interface, only a single mode of the PC is excited. These assumptions are usually satisfied in practical applications of the dispersion properties of PCs. Actually, for applications like superprism-based PC demultiplexer, beam collimating, and self-focusing, the required beam properties for proper operation of the device are more restrictive than our two assumptions here [18].

For the analysis of beam propagation in a two-dimensional PC, we use the geometry shown in Fig. 2. The polarization of the beam is assumed to be TE (electric field normal to the PC periodicity plane). A similar model can be developed for TM polarization. In addition, the interface of the PC and the incident medium is assumed to be parallel to one of the periodicity directions of the photonic crystal (for example, in Fig. 2 periodicities are in u and v directions, and the interface is along the u direction). Using Bloch theorem, a mode of this photonic crystal can be represented as

$$E_i = \sum_m \sum_n \tilde{E}_{mn} e^{jk_u u} e^{jk_v v} e^{jmK_u u} e^{jnK_v v} \tag{4}$$

where K_u and K_v are reciprocal lattice vectors corresponding to lattice periodicity directions u and v, respectively. The initial field profile along the u direction in the homogeneous incident medium at the interface (represented by $p(u)$) can be expressed as a spatial Fourier integral over wavevectors along the boundary, i.e.,

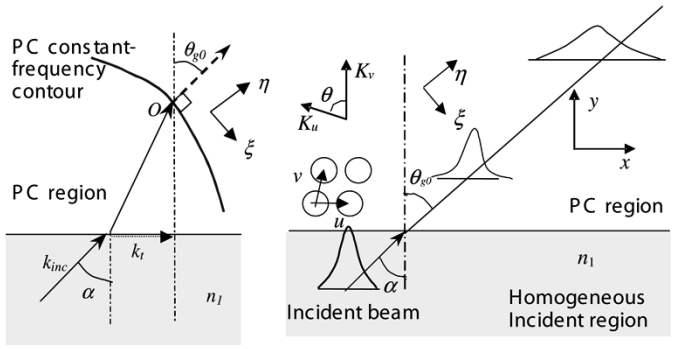

Fig. 2. Definition of various parameters when an optical beam is incident from a homogeneous region to a photonic crystal. (x, y) are the general Cartesian coordinates with x-axis parallel to the interface, and (u, v) are the lattice directions of the photonic crystal with u being along the interface and v (in general) at an angle θ with respect to the interface. Coordinates (ξ, η) are defined for each point of the band structure with η representing the direction of propagation (normal to the constant frequency contour or along the direction of group velocity, shown with the dashed arrow) and ξ being perpendicular to the direction of propagation. K_u and K_v are reciprocal lattice vectors of the photonic crystal [32] corresponding to u and v lattice vectors, respectively. In the text, beam profile along planes parallel to the boundary (as shown in this figure) is analyzed.

$$p(u) = \int_{k_u} A(k_u) \exp(jk_u u)\, dk_u. \tag{5}$$

Using (5), an incident beam can be considered as the superposition of infinite number of plane waves. Note that in a 2-D propagation plane in the incident homogeneous bulk medium, a plane wave can be characterized by only one component of its wavevector (since $|\bar{k}| = n_1\omega/c$). For each plane-wave component in the incident medium (i.e., each k_u), we can find a corresponding transmission coefficient that relates the plane wave to its corresponding PC mode excited inside the PC. Note that we have assumed that only a single propagating PC mode is excited for each incident plane-wave component $\exp(jk_u u)$. The excitation of a PC mode by this incident plane-wave component can be represented as

$$\exp(jk_u u) \rightarrow t(k_u) \sum_m \sum_n \tilde{E}_{mn} e^{jk_u u} e^{jk_v v} e^{jmK_u u} e^{jnK_v v} \tag{6}$$

where the right-hand side represents the excited PC mode. In (6), $t(k_u)$ is the amplitude transmission coefficient corresponding to the incident plane-wave component represented by k_u. Note that in this representation, we have considered only a single propagating PC mode (following our initial assumptions). Moreover, evanescent components have been deliberately dropped since we are only interested in propagating behavior of the beam rather than its behavior close to the interface. Nevertheless, the evanescent modes are taken into account in calculating the transmission coefficient $t(k_u)$ from the incident medium to the PC region. At a single value of v, we may rewrite (6) as

$$\exp(jk_u u) \rightarrow t'(k_u) \sum_m \left(\frac{\tilde{E}'_m}{\tilde{E}'_0} \right) e^{jk_u u} e^{jmK_u u} \tag{7}$$

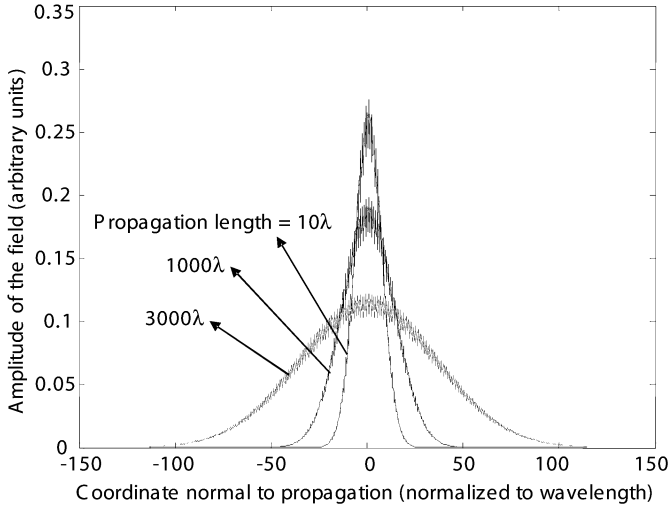

Fig. 3. Beam profile for a Gaussian beam normally incident on a square lattice PC (air holes in Si, $r/a = 0.4$) at different propagation lengths inside the PC. The incident beam used in the simulation was a Gaussian beam with beamwidth (full-width at half-maximum) of 20λ (TE polarization at $a/\lambda = 0.3$).

where $\tilde{E}'_m = \sum_n \tilde{E}_{mn} \exp(jk_v v) \exp(jnK_v v)$ and $t'(k_u) = t(k_u)\tilde{E}'_0$. We also define $\tilde{a}_m = \tilde{E}'_m/\tilde{E}'_0$. By combining (5) and (7) and using the linearity of the beam propagation, we can get

$$p(u) = \int_{k_u} A(k_u) \exp(jk_u u) dk_u \rightarrow \int_{k_u} A(k_u) t'(k_u) \sum_m \tilde{a}_m e^{jk_u u} e^{jmK_u u} dk_u = p_{\mathrm{PC}}(u) \tag{8}$$

where $p_{\mathrm{PC}}(u)$ represents the beam shape inside the PC at the interface. When the spectral bandwidth of the input beam is relatively small, the transmission coefficient is almost constant in the spectral range of the input beam resulting in

$$\begin{aligned} p_{\mathrm{PC}}(u) &\approx t'(k_{u0}) \int_{k_u} A(k_u) \sum_m \tilde{a}_m e^{jk_u u} e^{jmK_u u} dk_u \\ &= t'(k_{u0}) \sum_m \tilde{a}_m e^{jmK_u u} \int_{k_u} A(k_u) e^{jk_u u} dk_u \\ &= t'(k_{u0}) \sum_m \tilde{a}_m e^{jmK_u u} p(u) \end{aligned} \tag{9}$$

where k_{u0} represents the center spatial frequency of the beam. Using the fact that $\tilde{a}_0 = 1$, we obtain

$$p_{\mathrm{PC}}(u) \approx t'(k_{u0}) \left(1 + \sum_{m \neq 0} \tilde{a}_m e^{jmK_u u}\right) p(u) \tag{10}$$

for the beam inside the PC right at the interface.

For beams with a narrow spectral content, the (spatial) spectral bandwidth of $p(u)$ is smaller than K_u. Therefore, the original beam profile inside the PC region is modulated by a high-frequency pattern due to $\tilde{a}_m e^{jmK_u u}$ terms in (10). However, the envelope of the beam, which determines the large-scale beam profile that we are interested in, has the same features as the original incident beam $p(u)$.

In Fig. 3, the results for the exact simulation of the properties of a Gaussian beam incident on a square lattice photonic crystal at different propagation lengths inside the PC region are shown. These simulations were performed using a combination of plane-wave expansion and mode-matching techniques. It can be observed from Fig. 3 that the envelope of the beam inside the PC even after large propagation lengths still remains Gaussian. The high-frequency modulation of the beam profile is also clear in Fig. 3.

After addressing the transmission properties at the boundary, we now consider the propagation of the beam inside the PC. We assume, as shown in Fig. 2, that the input beam excites PC modes around point O in the band structure. We define ξ and η as the coordinates in directions tangent and normal to the constant frequency contour at point O (Fig. 2). Thus, the direction of group velocity (or wave propagation) at point O is along the η direction.

Assume we have an initial distribution $p_1(x)$ along $y = y_1$ (i.e., a line parallel to the x-axis) inside the PC. Note that x and y are the general coordinate variables and that x and u are parallel to the interface but v and y are not necessarily parallel. We can expand this distribution over photonic crystal modes as

$$\begin{aligned} p_1(x) &= \int A(k_x) U_{k_x}(x, y_1) \exp(jk_x x) \exp(jk_y y_1)\, dk_x \\ &= \int A(k_x) \\ &\quad \times \left(\sum_m \sum_n \tilde{E}_{mn}(k_x) \right. \\ &\qquad \left. \times \exp(jm\bar{K}_u \cdot \bar{r}) \exp(jn\bar{K}_v \cdot \bar{r}) \right) \\ &\quad \times \exp(jk_x x) \exp(jk_y y_1)\, dk_x \\ &= \int A(k_x) \\ &\quad \times \left(\sum_m \sum_n \tilde{E}_{mn}(k_x) \right. \\ &\qquad \times \exp[j(k_x - mK_u \sin\theta)x] \\ &\qquad \left. \times \exp[j(k_y + mK_u \cos\theta + nK_v)y_1] \right) dk_x \end{aligned} \tag{11}$$

where reciprocal lattice vectors [32],

$$\begin{cases} \bar{K}_u = -\hat{x} K_u \sin\theta + \hat{y} K_u \cos\theta \\ \bar{K}_v = \hat{y} K_v \end{cases} \tag{12}$$

are used in the last equality in (11). The spatial Fourier transform of the field distribution can be calculated as

$$\begin{aligned} P_1(k) &= \int p_1(x) \exp(-jkx)\, dx \\ &= \int e^{-jkx} \int A(k_x) \\ &\quad \times \left(\sum_m \sum_n \tilde{E}_{mn}(k_x) \right. \\ &\qquad \times \exp[j(k_x - mK_u \sin\theta)x] \\ &\qquad \left. \times \exp[j(k_y + mK_u \cos\theta + nK_v)y_1] \right) dk_x dx \\ &= \int A(k_x) \sum_m \sum_n \tilde{E}_{mn}(k_x) \\ &\quad \times \exp[j(k_y + mK_u \cos\theta + nK_v)y_1] \\ &\quad \times \int e^{-jkx} \exp[j(k_x - mK_u \sin\theta)x]\, dx\, dk_x \end{aligned} \tag{13a}$$

which can be simplified as

$$\begin{aligned} P_1(k) &= \int A(k_x) \sum_m \sum_n \tilde{E}_{mn}(k_x) \\ &\quad \times \exp[j(k_y + mK_u \cos\theta + nK_v)y_1] \\ &\quad \times \delta(-k + k_x - mK_u \sin\theta)\, dk_x \\ &= \sum_m \sum_n A(k_x)\tilde{E}_{mn}(k_x) \\ &\quad \times \exp\{j[k_y(k_x) + mK_u \cos\theta \\ &\quad + nK_v]y_1\}\,|_{k_x = k + mK_u \sin\theta} \end{aligned} \tag{13b}$$

or

$$\begin{aligned} P_1(k) = \sum_m \sum_n & A(k + mK_u \sin\theta)\tilde{E}_{mn}(k + mK_u \sin\theta) \\ & \times \exp[jk_y(k + mK_u \sin\theta)y_1] \\ & \times \exp(jnK_v y_1). \end{aligned} \tag{14}$$

Note that k_y is a function of k_x [i.e., $k_y = k_y(k_x)$] which reflects the effect of the PC band structure in the actual beam shape during the propagation inside the PC. We now assume that the spectral content of the beam profile is bandlimited around $k = k_{x0}$ and express the beam profile as a baseband portion (which will be called envelope from now on, since it contains the information that defines the envelope of the beam) multiplied by $\exp(jk_{x0}x)$. In order to calculate the envelope of the beam, we must filter out the high-frequency variations [as described by $m \neq 0$ terms in (10) and graphically shown in Fig. 3]. We also need to shift the spectrum of the filtered beam by $k = -k_{x0}$ to exclude the $\exp(jk_{x0}x)$ term. Starting with the beam spectrum given in (14) and assuming that the incident beam (or the envelope inside the PC) is bandlimited to the interval of $[k_{x0} - K_u \sin\theta/2, k_{x0} + K_u \sin\theta/2]$, we can eliminate all terms with $m \neq 0$ in (14) to filter out the high-frequency portions. The resulting spectrum is

$$P_{1,\text{filt}}(k) = A(k)\exp[jk_y(k)y_1] \sum_n \tilde{E}_{0n}(k)\exp(jnK_v y_1) \tag{15}$$

for $k_{x0} - K_u \sin\theta/2 < k < k_{x0} + K_u \sin\theta/2$. The envelope of the beam at point 1 inside the PC, denoted as $\bar{P}_1(k)$, is then calculated by shifting the $P_{1,\text{filt}}(k)$ by $k = k_{x0}$. The result is

$$\begin{aligned} \bar{P}_1(k) = A(k + k_{x0})\exp[jk_y(k + k_{x0})y_1] \\ \times \left(\sum_n \tilde{E}_{0n}(k + k_{x0})\exp(jnK_v y_1) \right) \end{aligned} \tag{16}$$

for $-K_u \sin\theta/2 < k < K_u \sin\theta/2$. Now if we consider the same beam at the plane $y = y_2$, we have

$$\begin{aligned} \bar{P}_2(k) = A(k + k_{x0})\exp[jk_y(k + k_{x0})y_2] \\ \times \left(\sum_n \tilde{E}_{0n}(k + k_{x0})\exp(jnK_v y_2) \right) \end{aligned} \tag{17}$$

for $-K_u \sin\theta/2 < k < K_u \sin\theta/2$. If $y_2 - y_1 = 2\pi l/K_v$ (with l being an integer), then

$$\bar{P}_2(k) = \bar{P}_1(k)\exp[jk_y(k + k_{x0})(y_2 - y_1)] \tag{18}$$

which means that the effect of propagation from $y = y_1$ to $y = y_2$ can be represented as a phase change in spectral domain similar to plane-wave-type propagation with propagation constant k_y. Thus, the main effect of propagation in PCs on the beam envelope is the phase variations of PC modes from initial plane to the observation plane.

Based on (18), we can write the propagation transfer function of the structure from $y = y_1$ to $y = y_2$ plane as

$$H(k) = \frac{\bar{P}_2(k)}{\bar{P}_1(k)} = \exp[jk_y(y_2 - y_1)] \tag{19}$$

where $k_y = k_y(k_x)$ is related to k_x through the dispersion relation of the structure at the constant temporal frequency of the beam. The relation is exactly the same if we monitor the propagation in a bulk medium. Based on this similarity, we extend the relation for a beam propagating in the bulk medium along the η direction (Fig. 2) to the photonic crystal case, and write the propagation relation for the beam propagating along the direction η as

$$H(k_\xi) = \frac{\bar{P}_2(k_\xi)}{\bar{P}_1(k_\xi)} = \exp[-jk_\eta(k_\xi)(\eta_2 - \eta_1)] \tag{20}$$

where ξ is the coordinate axis normal to η as shown in Fig. 2. Now, we can approximate the transfer function by the first three terms of its Taylor expansion

$$H(k_\xi) = \exp\{-j[\Phi_0 + (k_\xi - k_{\xi 0})\Phi_1 + (k_\xi - k_{\xi 0})^2\Phi_2]\} \tag{21a}$$

where we have

$$\Phi_0 = (\eta_2 - \eta_1)k_\eta(k_{\xi 0}) \tag{21b}$$

$$\Phi_1 = (\eta_2 - \eta_1)\left.\frac{\partial k_\eta}{\partial k_\xi}\right|_{k_\xi = k_{\xi 0}} = 0 \tag{21c}$$

$$\Phi_2 = \frac{1}{2}(\eta_2 - \eta_1)\left.\frac{\partial^2 k_\eta}{\partial k_\xi^2}\right|_{k_\xi = k_{\xi 0}}. \tag{21d}$$

Note that the linear term coefficient in (21-c) is zero because of the particular choice of the coordinates (ξ, η) with η being in the direction of propagation. The chirp parameter (b) [31] is defined as

$$b = \Phi_2 = \frac{1}{2}(\eta_2 - \eta_1)\left.\frac{\partial^2 k_\eta}{\partial k_\xi^2}\right|_{k_\xi = k_{\xi 0}}. \tag{22}$$

The chirp parameter is essentially responsible for broadening of the beam during propagation. If we define $\Theta(k_\xi) = (\partial k_\eta/\partial k_\xi)|_{k_\xi}$, then the angle of group velocity

direction (i.e., normal to the constant frequency contour) with respect to the normal to the interface of the PC and the incident medium (see Fig. 2) can be written as

$$\theta_g(k_\xi) = \theta_{g0} + \tan^{-1}(\partial k_\eta / \partial k_\xi) \tag{23}$$

where θ_{g0} is the angle of group velocity for $k_{\xi 0}$, as shown in Fig. 2. Since $\Theta(k_{\xi 0}) = 0$, due to the definition of the direction of group velocity, it is found that

$$\left.\frac{\partial \theta_g}{\partial k_\xi}\right|_{k_\xi = k_{\xi 0}} = \left.\left(\frac{1}{1+\Theta^2}\frac{\partial \Theta}{\partial k_\xi}\right)\right|_{k_\xi = k_{\xi 0}} = \left.\frac{\partial^2 k_\eta}{\partial k_\xi^2}\right|_{k_\xi = k_{\xi 0}}. \tag{24}$$

Therefore

$$b = \frac{1}{2}(\eta_2 - \eta_1)\left.\frac{\partial \theta_g}{\partial k_\xi}\right|_{k_\xi = k_{\xi 0}} \tag{25}$$

which suggests that the diffraction property of the medium depends basically on the local value of $\partial \theta_g / \partial k_\xi$ (or equivalently, the curvature of the constant frequency contour) in the 2-D k -plane. For a bulk homogeneous medium with refractive index n and free-space wavevector k_0, direct calculations result in

$$\left.\left(\frac{\partial \theta_g}{\partial k_\xi}\right)\right|_{k_\xi = k_{\xi 0}} = \frac{1}{k_0 n}. \tag{26}$$

We use this relation to define effective diffraction index of the PC medium (this can be similarly extended to any other medium) as

$$n_e = \frac{1}{k_0 (\partial \theta_g / \partial k_\xi)|_{k_\xi = k_{\xi 0}}}. \tag{27}$$

Noting that $(\partial k_t / \partial k_\xi)|_{k_\xi = k_{\xi 0}} = \cos\theta_{g0}$ and $k_t = n_1 k_0 \sin\alpha$ (k_t is the component parallel to the interface in the incident bulk medium with index n_1, as shown in Fig. 2), (27) can be rewritten as

$$n_e = \frac{1}{k_0 (\partial \theta_g / \partial k_t)_0 \cos\theta_{g0}} = \frac{n_1 \cos\alpha}{(\partial \theta_g / \partial \alpha)_0 \cos\theta_{g0}} \tag{28}$$

in which subscript "0" is used to emphasize that these values are local values calculated at the point for which Taylor expansion is written (i.e., at $k_\xi = k_{\xi 0}$). Note that both magnitude and sign of n_e are important. The magnitude determines how much phase chirp is added to the beam, and the sign is either positive (positive chirp, as in ordinary dielectric media) or negative (negative chirp). The negative chirp has no counterpart in conventional wave propagation in a bulk dielectric medium and can be used to compensate for the effect of ordinary diffraction. If the assumptions for the above derivation are satisfied, the effective index model can be used for describing all the properties (for example diffraction) of beam propagation inside PCs using only the beam envelope. This provides better understanding of wave propagation phenomena in PCs and eliminates the need for long direct numerical electromagnetic simulations. The concept of effective index defined in (27)–(28) is different from other effective indexes defined previously such as phase refractive index and group velocity effective index [30]. Phase refractive index defined by the phase velocity of the main Bloch component of the PC mode does not carry much physical information in strongly modulated media [30], and group velocity effective index, defined for a certain direction, describes how fast energy is transferred in that direction [30]. The effective index defined in this paper deals with diffraction of optical beams and is defined using the curvature of bands at a certain frequency (considering PC modes in the vicinity of the excitation point). The usefulness of such definition lies in its ability to describe the behavior of the envelope of the optical beam as it propagates through the periodic structure, a concept that has immediate application in modeling and design of photonic devices made based on dispersion properties of PCs outside the PBG.

V. Applications of the Effective Index Model

A. Propagation of Gaussian Beams in PCs

As the first example, we consider here the propagation of a Gaussian beam [33] inside a PC. Fig. 3 shows the exact simulation (using modal approach based on plane-wave expansion and mode matching) of the beam profile inside the PC at different propagation lengths for an incident Gaussian beam with beamwidth 20λ with its waist located at the interface in air. Fig. 3 shows that the beam inside the PC has a Gaussian envelope with high-frequency modulations due to the periodic PC structure. In practical applications, we are more interested in the beam envelope than its high-frequency modulation. The effective index model is helpful in analyzing such cases.

Fig. 4 shows the beam profile inside the PC at different propagation lengths for an incident Gaussian beam calculated using the exact simulations and using the effective index model. Figs. 4(a)–(c) correspond to different incident beam waists ($10\lambda, 20\lambda$, and 50λ, respectively). The PC structure is a 2-D square lattice of air-holes in Si ($\varepsilon_r = 11.4$) with hole radius of $r = 0.40a$, where $a = 0.3\lambda$ is the lattice period. Fig. 4 shows that the beam envelope in all cases is successfully calculated from the effective index model, and in all these cases, the Gaussian feature of the beam envelope is preserved during propagation inside the PC. Fig. 4(d) shows the variation of the Gaussian beamwidth with the propagation length (L) inside the PC. Fig. 4 shows that the large scale parameters of the beam obtained by direct simulations are in agreement with those obtained by fitting Gaussian beam characteristics into the data from the direct simulations (to make sure that Gaussian beam approximation is valid everywhere inside the PC) as well as those obtained from the simplified effective index model.

B. Diffraction Compensation in PCs

We have shown that for propagation through a PC the diffraction behavior is governed by the dispersion of the PC. Note that we can modify the photonic band structure of the PC by

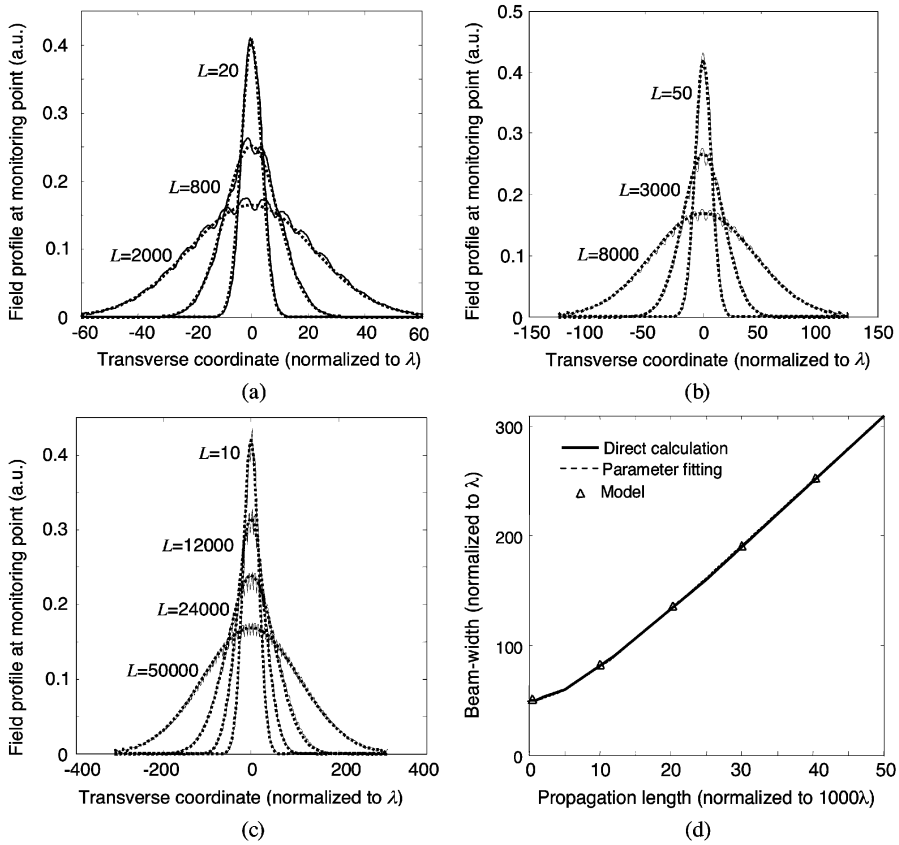

Fig. 4. Beam profiles (normal to the direction of propagation) for propagation of a Gaussian beam through a square lattice photonic crystal (air-holes in Si, $r/a = 0.4$ at normalized temporal frequency $\omega_n = a/\lambda = 0.3$) for different propagation lengths (L) inside the PC. The polarization of the beam is TE, and the initial beamwidths (at $L = 0$) are (a) 10λ, (b) 20λ, and (c) 50λ. Solid lines are the results of exact simulations using plane-wave expansion technique, and dotted lines are those calculated from the effective index model. In (d) the beamwidth variation with propagation length inside the PC for the beam parameters as in (c) is shown.

changing its properties (e.g., lattice type, size of the holes, shape of the holes, etc.) or by choosing the proper point on the band structure to have the desired features. Thereby, the diffraction properties of the beam propagation in photonic crystals (as long as they satisfy the corresponding assumptions) can be controlled by designing the PC structure using the effective index model.

Fig. 5 shows the results for the propagation of a TE polarized Gaussian beam $(a/\lambda = 0.30)$ through a two-stage PC composed of two square lattices of air-holes in Si with $r_1/a = 0.40$ and $r_2/a = 0.35$ with the same lattice constant [shown in Fig. 5(a)]. The first PC region has a positive effective index. Thus, the propagation through the first PC region adds a quadratic phase to the signal, which results in broadening of the beam. The resulting beam then enters into the second PC region, which is designed to have a negative effective index. As a result, the quadratic phase term in the second region after some propagation length cancels that introduced by propagation through the first region. The variations of the beamwidth of the Gaussian beam in the first and the second PC regions are shown in Fig. 5(b) and (c), respectively. As seen in Fig. 5, the original beamwidth is retrieved at $y = y_2$ using the propagation in the second PC. Further propagation in the second region adds more quadratic phase, which broadens the beam again. This effect has been observed earlier, and was attributed to the negative refraction of the photonic crystal [34], but as we have shown here, it is related to the negative curvature of the bands of the PC and can occur in both positive and negative refraction regions.

VI. Discussion

The steps that must be taken to find the effective index for a PC at a specific frequency and a specific direction of propagation (i.e., a specific point in the k-space) are as follows. At first the band structure must be calculated in the form of constant frequency contours. In this paper, we used 2-D simulations (based on plane-wave expansion method) to calculate the band structure of a 2-D PC. For a three-dimensional (3-D) PC or a slab of 2-D PC with finite thickness, 3-D simulations must be used. However, the rest of the steps to find the effective index of the PC are the same in all cases. In the second step, the operation point in the PC band structure (as described by the temporal frequency ω and the propagation direction (coordinates in k-space) must be found. In the third step, the effective index at the operating point can be calculated using (27) or (28). The temporal and spatial bandwidth of the incident signal must be taken into account in justifying the conditions for which the model is valid.

The results shown in previous sections suggest that the effective index model is a powerful tool for the analysis of beam propagation in PCs. For successful application of this model, the assumptions behind the derivation of the effective index must

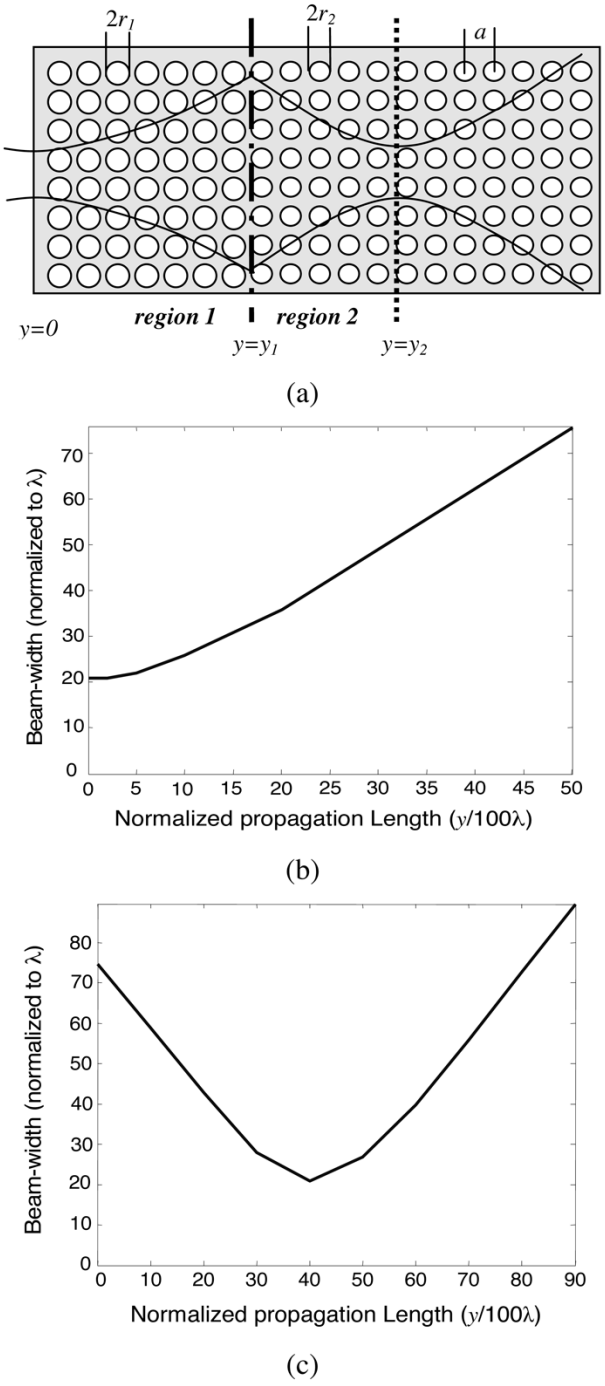

Fig. 5. Beamwidth variations for a Gaussian beam propagating in a two stage photonic crystal structure. (a) Schematics of beam variations inside the structure. (b) Beamwidth in a square lattice of air-holes in Si $(r_1/a = 0.40)$, and (c) beamwidth of resulting beam from (a) in a square lattice of air-holes in Si $(r_2/a = 0.35)$. The initial width of the Gaussian beam entering region 1 at $y = 0$ is 20λ, $a/\lambda = 0.30$, and TE polarization is considered.

be carefully validated. The errors in using this model can come from the following sources.

A. Higher Order Spectral Phase Terms in the Taylor Expansion of the Transfer Function (21a)

These terms come into the picture when the variation of the band structure in the operation region (as defined by the spatial and temporal frequency content of the incident beam) is so rapid that the higher order spectral phase terms in the Taylor expansion cannot be neglected.

Qualitatively, the effect of third-order and fourth-order spectral phase terms can be included similar to time-domain effects [31]. The effect of third-order spectral phase can be considered as a quadratic chirp. For the case of a Gaussian beam, this quadratic chirp results in a nonsymmetric beam profile with oscillations on one side [31]. Quantitatively, these effects can be directly included in the propagation transfer function. As an example, the equally spaced side-lobes for the beam propagating in a square lattice reported previously [22] can be easily modeled by approximating the band structure using a combination of second-order and fourth-order spectral phase terms.

B. Cutoff

Cutoff occurs when part of the beam spectrum does not go through the PC structure because of the absence of a corresponding propagating mode inside the PC. In other words, some incident spatial frequencies are suppressed due to their inability to excite propagating PC modes. The effect of cutoff can be easily understood from a Fourier-domain point of view. Some parts of the spatial frequency content of the beam are filtered out, and as a result, the beam profile will be symmetrically or nonsymmetrically broadened (depending on what part of the spatial frequency domain is cut).

C. Transmission Nonuniformity

Unlike (9) and (10), if the transmission coefficient from the incident medium to the PC region varies considerably within the incident beam spectrum, the transmission coefficients ($t'(k_u)$ in (8)) for different incident plane-wave components (or different incident spatial frequencies) are not equal, and the corresponding effect should be taken into account. This may include both magnitude and phase of the transmission coefficient.

The effect of transmission nonuniformity according to (8) appears as a direct filtering of the input beam spectrum. In other words, the input beam from the incident medium is transferred into the PC by a filtering process defined by the transmission coefficient $t'(k_x)$. Once this coefficient is calculated for different incident angles, the effect can be readily included. In the basic case described before, this value is assumed to be slowly varying in the spatial bandwidth of the incident beam and the net effect was considered as a constant multiplication factor independent of spatial frequency. We can integrate the effect of cutoff and transmission nonuniformity into a single input transfer function $H_{\rm in}(k_x)$. The propagation transfer function can easily be calculated from the band structure using its Taylor expansion terms (as before) $H_{\rm pr}(k_x; l)$, where l is the propagation length. The overall transfer function $H(k_x) = H_{\rm in}(k_x)H_{\rm pr}(k_x; l)$ governs the resulting beam profile in the spectral domain. Note that in cases B and C, the effective index model can still be used for the analysis of the propagation of the excited PC modes through the PC.

D. Multimode Excitation Inside the PC

When some plane-wave components of the incident beam excite more than one PC mode with comparable strength, the ef-

fective index model cannot be used directly. The reason is that this model cannot provide any information about the relative strengths of different modes excited in the structure. Nevertheless, if we find the coupling coefficient of incident beam to these modes, the behavior can be modeled by considering the propagation of each beam separately (with its corresponding effective index). The beam profile at each point can be obtained by superposition of these beams.

As an example, consider the propagation of an optical beam through a 2-D square lattice photonic crystal of air-holes (with normalized radius $r/a = 0.30$) in silicon ($\varepsilon_r = 11.4$). The incident beam is Gaussian with TE polarization at normal angle to the PC region. The incident region is assumed to have $\varepsilon_r = 11.4$, and normalized frequency of operation is $\omega_n = a/\lambda = 0.3$. Fig. 6(a) shows contours of absolute value of the effective index for this PC calculated from (27). The constant frequency contour corresponding to the frequency of operation and the wavevector representing the excited PC mode (dashed arrow) are also plotted in Fig. 6(a). It can be seen from Fig. 6(a) that the effective index for $\omega_n = 0.3$ at normal incidence (the geometry of the structure is the same as that introduced in Fig. 2 for which normal incidence corresponds to $k_x = 0$) is $n_e = 0.4$. To investigate the accuracy of this value for the effective index, we directly simulated the propagation of Gaussian beams with different beamwidths (thus different spatial bandwidths) and extracted the value of the effective index for each case by curve fitting. Fig. 6(b) shows the variation of calculated effective index (from direct simulations) versus the incident beamwidth. The calculated effective index clearly approximates the theoretical value predicted by effective index model as larger beamwidths (or equivalently, beams with narrower spatial spectrum) are used. The difference between the actual effective index and that calculated using our effective index model becomes larger as the incident beam waists become smaller, and the difference is more than 10% for beam waists less than 4λ for this special case. In Fig. 6(c) the variations of beamwidth inside the PC region versus the propagation length are shown for different incident beam waists and compared with that of a Gaussian beam propagating in an ordinary bulk medium. It is clearly observed from Fig. 6(c) that the propagation behavior deviates more from its ideal Gaussian case as the incident beam waist becomes smaller. The reason is that for smaller beamwidths the beam has larger spatial frequency content and is affected more by limited spatial bandwidth of the PC ($|k_x a| < 0.4$) at the operation frequency ($\omega_n = 0.3$), referred to as cutoff, as well as by the presence of higher order terms of spectral phase due to variation of the effective index with the spatial frequency. Fig. 6(c) also suggests that for this special case, the effective index model has good accuracy for incident beam waists of at least $2w_0 = 4\lambda$.

The limitation obtained using Fig. 6 cannot be generalized to all PCs and all applications. The reason is that the propagation properties of PCs (cutoff, allowed spatial bandwidth, effective index variation, etc.) depend strongly on the PC structure, the temporal frequency of operation (i.e., ω_n), and the actual operation region in the band structure (i.e., the spatial frequency range of operation). For most practical applications of

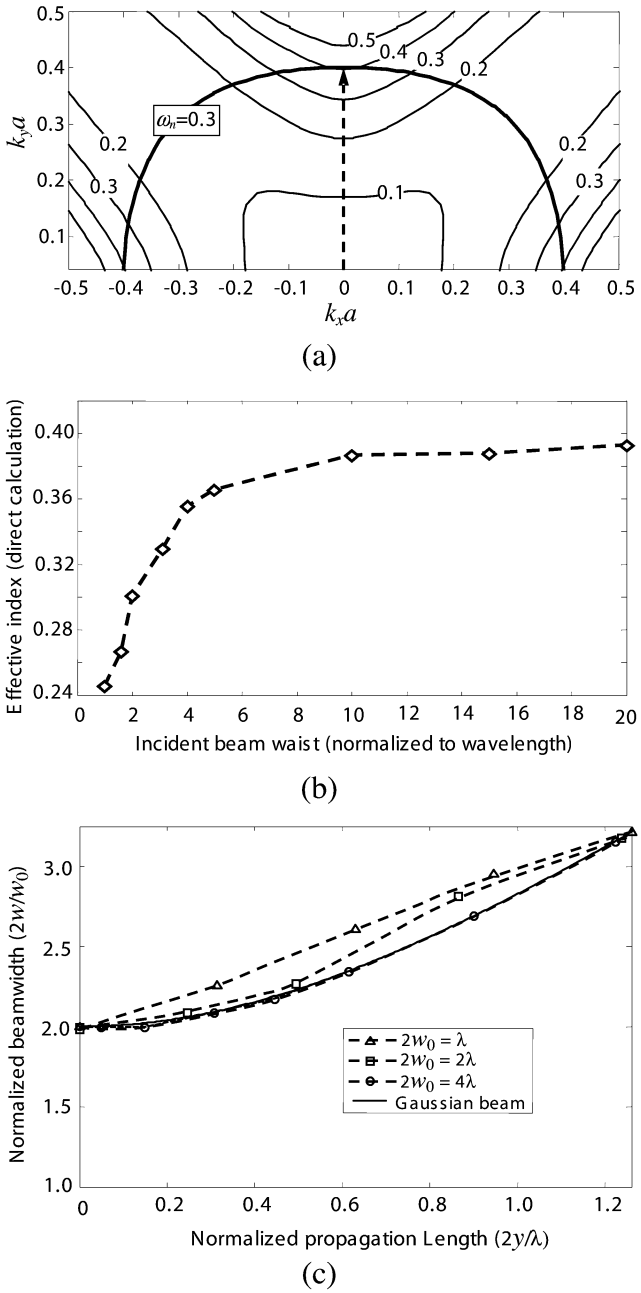

Fig. 6. A 2-D square lattice PC with $r/a = 0.3$, and TE polarization is considered. (a) Contours of absolute value of the effective index calculated using (27) marked with their corresponding values; the constant temporal frequency contour for $\omega_n = 0.3$ is also shown in this figure. The dashed arrow corresponds to the PC mode with $\omega_n = 0.3$ and normal incidence, which is associated with an effective index of $n_e = 0.4$. (b) Effective indexes for different incident beamwidths calculated using direct simulation for propagation of a Gaussian beam. (c) Variations of beamwidth versus propagation length for different values of the incident beam waist are compared with that of a Gaussian beam in an ordinary bulk medium.

dispersion properties of PCs (superprism demultiplexing, self-focusing, diffraction control, etc.), the optical beam size is much larger than the wavelength, for which the effective index model can be used with good accuracy.

It is important to note that the assumptions for the validity of the effective index model are usually satisfied in practical applications of the dispersion properties of PCs. For example, in

designing a demultiplexer using superprism effect [16], the incident beam must have a small divergence angle (i.e., small spatial frequency content) to avoid very large structures [16], [18]. Furthermore, the beams at different wavelengths inside the PC must have minimal crosstalk, which requires single-mode PC excitation as well as relatively smooth band structure behavior. Similar arguments hold for the case of diffraction-controlling PC devices. The details of the design and optimization of superprism-based demultiplexers using the effective index model have been published before [18], and thus not included in Section V of this paper.

Another issue to be considered is that although the majority of the considerations in this paper were on two-dimensional photonic crystals, we can use exactly the same method to analyze the beam propagation behavior for a three-dimensional photonic crystal (or a slab of 2-D PC). Also, by calculating the two-dimensional band structure of a one-dimensional PC, we can find its effect on a two-dimensional beam profile.

VII. Conclusion

To conclude, using the analogy between beam propagation in space-domain and pulse propagation in the time-domain, a simple model is provided to describe the beam propagation through a photonic crystal. Based on this model, the diffraction properties of a photonic crystal can be directly extracted from its band structure eliminating the need to run elaborate simulations such as FDTD or BPM. In addition, the simplified model for diffraction gives insight into what an optical beam undergoes while it propagates through a photonic crystal structure, and makes the design of such structures much easier. The effective index model is a powerful tool for studying beam propagation effects inside PCs. Using this model we showed that PCs can be used to control diffraction of optical beams. Diffraction compensation and diffraction-free propagation can be achieved by appropriately designing the PC structure through the choice of lattice type, the geometry of holes in a unit cell, and the excitation point in the band structure.

We also discussed the assumptions that must be satisfied for the validity of the effective index model. For practical applications of dispersion in PCs, these assumptions are usually valid and the results using this model agree very well with the accurate numerical simulations.

References

[1] E. Yablonovitch, "Inhibited spontaneous emission in solid-state physics and electronics," *Phys. Rev. Lett.*, vol. 58, no. 20, pp. 2059–2062, May 1987.

[2] S. John, "Strong localization of photons in certain disordered dielectric superlattices," *Phys. Rev. Lett.*, vol. 58, no. 23, pp. 2486–2489, Jun. 1987.

[3] J. Joannopoulos, R. Meade, and J. Winn, *Photonic Crystals: Molding the Flow of Light*. Princeton, NJ: Princeton Univ. Press, 1995.

[4] S. Fan, A. Mekis, S. G. Johnson, and J. D. Joannopoulos, "Manipulating light with photonic crystals," in *AIP Conf. Proc.*, vol. 560, 2001, pp. 57–76.

[5] M. Loncar, D. Nedeljkovic, T. Doll, J. Vuckovic, A. Scherer, and T. P. Pearsall, "Waveguiding in planar photonic crystals," *Appl. Phys. Lett.*, vol. 77, pp. 1937–1939, Sep. 2000.

[6] O. Painter, J. Vuckovic, and A. Scherer, "Defect modes of a two-dimensional photonic crystal in an optically thin dielectric slab," *J. Opt. Soc. Amer. B*, vol. 16, pp. 275–285, Feb. 1999.

[7] A. V. Andreev, A. V. Balakin, I. A. Ozheredov, A. P. Shkurinov, P. Masselin, G. Mouret, and D. Boucher, "Compression of femtosecond laser pulses in thin one-dimensional photonic crystals," *Phys. Rev. E*, vol. 63, p. 016 602, Dec. 2000.

[8] N. I. Koroteev, S. A. Magnitskii, A. V. Tarasishin, and A. M. Zheltikov, "Compression of ultrashort light pulses in photonic crystals: When envelopes cease to be slow," *Optics Commun.*, vol. 159, pp. 191–202, Jan. 1999.

[9] I. V. Shadirvov, A. A. Sukhorukov, and Y. S. Kivshar, "Beam shaping by a periodic structure with negative refraction," *Appl. Phys. Lett.*, vol. 82, pp. 3820–3822, Jun. 2003.

[10] R. Morandotti, H. S. Eisenberg, Y. Silberberg, M. Sorel, and J. S. Aitchison, "Self-focusing and defocusing in waveguide arrays," *Phys. Rev. Lett.*, vol. 86, pp. 3296–3299, Apr. 2001.

[11] T. Pertsch, T. Zentgraf, U. Peschel, A. Brauer, and F. Lederer, "Beam steering in waveguide arrays," *Appl. Phys. Lett.*, vol. 80, pp. 3247–3249, May 2002.

[12] X. Yu and S. Fan, "Bends and splitters for self-collimated beams in photonic crystals," *App. Phys. Lett.*, vol. 83, pp. 3251–3253, Oct. 2003.

[13] H. Kosaka, T. Kawashima, A. Tomita, M. Notomi, T. Tamamura, T. Sato, and S. Kawakami, "Superprism phenomena in photonic crystals: Toward microscale lightwave circuits," *J. Lightw. Technol.*, vol. 17, no. 11, pp. 2032–2038, Nov. 1999.

[14] L. Wu, M. Mazilu, T. Karle, and T. F. Krauss, "Superprism phenomena in planar photonic crystals," *IEEE J. Quantum Electron.*, vol. 38, no. 7, pp. 915–918, Jul. 2002.

[15] L. Wu, M. Mazilu, and T. F. Krauss, "Beam steering in planar-photonic crystals: From superprism to supercollimator," *J. Lightw. Technol.*, vol. 21, no. 2, pp. 561–566, Feb. 2003.

[16] T. Baba and T. Matsumoto, "Resolution of photonic crystal superprism," *Appl. Phys. Lett.*, vol. 81, pp. 2325–2327, Sep. 2002.

[17] K. B. Chung and S. W. Hong, "Wavelength demultiplexers based on the superprism phenomena in photonic crystals," *Appl. Phys. Lett.*, vol. 81, pp. 1549–1551, Aug. 2002.

[18] B. Momeni and A. Adibi, "Optimization of superprism-based photonic crystal demultiplexers," *Appl. Phys. B*, vol. 6–7, pp. 555–560, Nov. 2003.

[19] H. Kosaka, T. Kawashima, A. Tomita, T. Sato, and S. Tawakami, "Photonic-crystal spot-size converter," *Appl. Phys. Lett.*, vol. 76, pp. 268–270, Jan. 2000.

[20] H. Kosaka, T. Kawashima, A. Tomita, M. Notomi, T. Tamamura, T. Sato, and S. Kawakami, "Self-collimation phenomena in photonic crystals," *Appl. Phys. Lett.*, vol. 74, pp. 1212–1214, Mar. 1999.

[21] D. N. Chigrin, S. Enoch, C. M. S. Torres, and G. Tayeb, "Self-guiding in two-dimensional photonic crystals," in *Proc. SPIE*, vol. 4655, Apr. 2002, pp. 63–72.

[22] J. Witzens, M. Loncar, and A. Scherer, "Self-collimation in planar photonic crystals," *IEEE J. Sel. Topics Quantum Electron.*, vol. 8, no. 6, pp. 1246–1257, Nov./Dec. 2002.

[23] D. N. Chigrin, S. Enoch, C. M. S. Torres, and G. Tayeb, "Self-guiding in two-dimensional photonic crystals," *Opt. Express*, vol. 11, pp. 1203–1211, May 2003.

[24] J. Witzens and A. Scherer, "Efficient excitation of self-collimated beams and single Bloch modes in planar photonic crystals," *J. Opt. Soc. Amer. A*, vol. 20, pp. 935–940, May 2003.

[25] M. Charbonneau-Lefort, E. Istrate, M. Allard, J. Poon, and E. H. Sargent, "Photonic crystal heterostructures: Waveguiding phenomena and methods of solution in an envelope function approximation," *Phys. Rev. B*, vol. 65, p. 125 318, Mar. 2002.

[26] A. Taflove, *Computational Electrodynamics. The Finite Difference Time-Domain Method*. Norwood, MA: Artech House, 1995.

[27] M. Koshiba, Y. Tsuji, and M. Hikari, "Time-domain beam propagation method and its application to photonic crystal circuits," *J. Lightw. Technol.*, vol. 18, no. 1, pp. 102–110, Jan. 2000.

[28] G. Tayeb and D. Maystre, "Rigorous theoretical study of finite-size two dimensional photonic crystals doped by microcavities," *J. Opt. Soc. Amer. A*, vol. 14, pp. 3323–3332, Dec. 1997.

[29] S. Boscolo and M. Midrio, "A fast algorithm for the simulation of propagation in large-area 2-D photonic crystal devices," *J. Lightw. Technol.*, vol. 20, no. 10, pp. 1869–1875, Oct. 2002.

[30] M. Notomi, "Theory of light propagation in strongly modulated photonic crystals: Refractionlike behavior in the vicinity of the photonic band gap," *Phys. Rev. B*, vol. 62, pp. 10 696–10705, Oct. 2000.

[31] R. Trebino, *Frequency-Resolved Optical Gating: The Measurement of Ultrashort Laser Pulses*. Norwell, MA: Kluwer Academic, 2000, ch. 2.

[32] N. W. Ashcroft and D. Mermin, *Solid State Physics*: International Thomson, 1976.

[33] J. T. Veredeyen, *Laser Electronics*. Englewood Cliffs, NJ: Prentice-Hall, 1995, ch. 3.

[34] M. Qiu, L. Thylén, M. Swillo, and B. Jaskorzynska, "Wave propagation through a photonic crystal in a negative phase refractive-index region," *IEEE J. Sel. Topics Quantum Electron.*, vol. 9, no. 1, pp. 106–110, Jan. 2003.

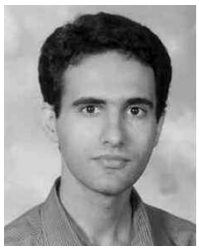

Babak Momeni (S'02) was born in Tehran, Iran, in 1977. He received the B.Sc. and M.Sc. degrees in electrical engineering from Sharif University of Technology, Tehran, Iran, in 1999 and 2001, respectively. He is currently working toward the Ph.D. degree at the Georgia Institute of Technology, Atlanta.

His research interests include wave propagation in periodic structures and analysis and applications of diffraction gratings.

Mr. Momeni is a Member of Eta Kappa Nu, the Optical Society of America (OSA), and the International Society for Optical Engineers (SPIE), Bellingham, WA.

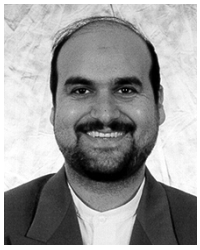

Ali Adibi (M'00–SM'04) was born in Shiraz, Iran, in 1967. He received the B.S.E.E. degree from Shiraz University in 1990, the M.S.E.E. degree from the Georgia Institute of Technology, Atlanta, in 1994, and the Ph.D. degree from the California Institute of Technology, Pasadena, in 1999. His Ph.D. research resulted in a breakthrough in persistent holographic storage in photorefractive crystals.

He worked as a Postdoctoral Scholar at the California Institute of Technology from 1999 to 2000. He has been an Assistant Professor in the School of Electrical and Computer Engineering, Georgia Institute of Technology, since 2000. His research interests include holographic data storage, holographic optical elements for optical communications, 3-D optical pattern recognition, design, characterization, and applications of photonic crystals for chip-scale WDM and biosensors, and optical communication and networking.

Dr. Adibi has been the Conference Chair for the Photonic Bandgap Materials and Devices Conference, PhotonicWest, since 2001, and the Program Chair for the Nanotechnology program, PhotonicWest, since 2002. He has served as a Technical Committee Member for several conferences, including the IEEE Lasers and Electro-Optics Society (LEOS) Annual Meeting. He has also been a Member of the Apker Award Selection Committee since 2002. He has been the recipient of numerous awards, including the Packard Fellowship (from the David and Lucile Packard Foundation), the National Science Foundation (NSF) Career Award, the Southeastern Center for Electrical Engineering Education (SCEEE) Young Faculty Development Award, the NASA Space Act Award, SPIE's Young Investigator Award, the Howard Ector Outstanding Teacher Award from the Georgia Institute of Technology, the Richard M. Bass Outstanding Teacher Award from the Georgia Institute of Technology, the Charles H. Wilts Prize for the best electrical engineering thesis of the year from the California Institute of Technology, the New Focus Student Award from the Optical Society of America (OSA), the Top Student (D. J. Lowell) Award from SPIE, and the Oscar P. Cleaver Award for the Outstanding Electrical Engineering Graduate Student of the Year, from the Georgia Institute of Technology. He is a Member of Sigma Xi, OSA, SPIE, and the Materials Information Society (ASM).